Phosphorus-31 and Carbon-13 Nuclear Magnetic Resonance Studies of Anaerobic Glucose Metabolism and Lactate Transport in *Staphylococcus aureus* Cells†

Fouad S. Ezra,* Donald S. Lucas, Robert V. Mustacich, and Anne F. Russell

ABSTRACT: High-resolution Fourier transform ^{31}P and ^{13}C nuclear magnetic resonance (NMR) has been used to probe several aspects of glucose metabolism and lactate transport in the Gram-positive bacterium *Staphylococcus aureus*. The ^{31}P NMR spectra show resonances due to intracellular (P_i^{in}) and extracellular orthophosphate (P_i^{ex}), sugar phosphate, and nucleoside di- and triphosphates. A peak due to teichoic acid has also been identified. Its appearance indicates a relatively high degree of mobility in the backbone of this cell wall polymer. The intracellular pH is estimated from the chemical shift of the P_i^{in} resonance and is found to be dependent upon the pH of the external medium. A prominent feature of the ^{31}P NMR spectra is the progressive broadening and downfield shift of the P_i^{in} resonance that occur when the cells are maintained in an anaerobic environment. Oxygenation causes a narrowing and an upfield shift of the P_i^{in} resonance, thereby reversing the trends observed under anaerobic conditions. These line width and chemical shift variations are attributed mainly to a binding of the orthophosphate to paramagnetic ions accumulated by the cells during growth. The ESR spectrum of a perchloric acid extract shows a sextet characteristic of Mn(II) hexaquo ions. It is suggested that the manganese is involved in oxygen metabolism. ^{13}C NMR spectra obtained from *S. aureus* cells incubated anaerobically with [1-^{13}C]- or [6-^{13}C]glucose show resonances due to fructose 1,6-bisphosphate as an intermediary metabolite and mannitol, lactate, and ethanol as the major end products of glucose metabolism. The identity of mannitol is determined from the ^{13}C NMR spectrum of a perchloric acid extract. It is demonstrated that the pH of the external medium affects the glycolytic rate and the distribution of end products. When the pH of the medium is raised from 6.0 to 7.5, the rate of glucose consumption is enhanced whereas the amount of mannitol produced relative to lactate is drastically reduced. The latter effect is explained in terms of the regulation of phosphofructokinase activity by the intracellular pH. The intra- and extracellular lactates appear as two well-resolved resonances due primarily to the presence of the manganous ions inside the cells. The result is a downfield shift and broadening of the intracellular resonance which depend on the oxygenation state of the cells and resemble the trends observed in the ^{31}P NMR spectra. The chemical shift inequivalence of the two lactate resonances allows the distribution and transport of this metabolite to be measured, with both the internal and external components being monitored independently. During anaerobic glycolysis, a lactate concentration gradient favoring the cytoplasmic compartment is established. The final intracellular concentration is estimated to be from 2 to 5 times greater than that in the external medium. In the presence of oxygen, lactate is transported into the cells. A rapid efflux occurs as the cells revert to an anaerobic state. Treatment with a fatty acid antimicrobial agent, octanoate, results in a concentration-dependent reduction of the transmembrane pH gradient and a loss of lactate from the cells during glycolysis. In addition, the uptake of lactate during oxygenation is completely inhibited.

High-resolution ^{31}P and ^{13}C nuclear magnetic resonance (NMR)[1] has been increasingly used in recent years to investigate various aspects of bioenergetics and metabolism in microorganisms. Much of this work has been summarized in several comprehensive reviews that have appeared in the literature during the past year (Kuchel, 1981; Roberts & Jardetzky, 1981; Scott & Baxter, 1981). By far, the most extensive series of NMR experiments were undertaken by Shulman and co-workers on the Gram-negative bacterium *Escherichia coli* (Ugurbil et al., 1978a,b, 1979, 1982). Such studies have been more recently extended by other investigators to a variety of protozoa and Gram-negative photosynthetic and nonphotosynthetic bacteria (Halpin et al., 1981; Runquist et al., 1981; Deslauriers et al., 1982; Kallas & Castenholtz, 1982; Mackenzie et al., 1982; Nicolay et al., 1982; Paalme et al., 1982). In all of these cases, NMR has provided information in a noninvasive and nondestructive manner on the cellular environment including intracellular pH and metal ion binding, on the identity and concentrations of intermediary and end products of metabolism, and on the pathways and kinetics of biochemical reactions as they occur in vivo.

In the present work, we have utilized a combination of ^{31}P and ^{13}C NMR to investigate metabolic processes in a Gram-positive facultative anaerobe *Staphylococcus aureus*. Previous ^{13}C and ^{15}N NMR studies of Gram-positive bacteria had focused only on the characterization of the cell wall components (Lapidot & Irving, 1979a,b). The importance of *S. aureus*, in particular, lies in its production of toxins and its associated pathogenicity in man (Cohen, 1972). Fundamental differences exist between this microorganism and *E. coli* and are highlighted in this report. These differences include the presence in *S. aureus* of teichoic acid as a component of the cell wall (^{31}P NMR) and the appearance of intracellular mannitol as an end product of glucose metabolism (^{13}C NMR).

† From the Procter & Gamble Company, Miami Valley Laboratories, Cincinnati, Ohio 45247. *Received January 19, 1983.*

[1] Abbreviations: NMR, nuclear magnetic resonance; ESR, electron spin resonance; P_i, orthophosphate; NTP, nucleoside triphosphate; NDP, nucleoside diphosphate; NAD, nicotinamide adenine dinucleotide; L, lactate; EDTA, ethylenediaminetetraacetate; Fru-1,6-P_2, fructose 1,6-bisphosphate; Fru-6-P, fructose 6-phosphate; Glc-6-P, glucose 6-phosphate; PFK, phosphofructokinase; Mno-1-P, mannitol 1-phosphate; MDH, mannitol-1-phosphate dehydrogenase. P_i and L refer either to the metabolites or to their respective NMR resonances. The terms are used interchangeably in the text.

0006-2960/83/0422-3841$01.50/0

We have addressed several interrelated aspects of anaerobic glucose metabolism in *S. aureus* such as the distribution of end products, the rate of glycolysis, lactate transport, and the effects of pH on these processes. Within this context, the present work also deals with the mode of action of an antimicrobial agent, octanoate. This medium-chain saturated fatty acid functions in a manner similar to the well-known uncoupler 2,4-dinitrophenol (DNP) by transporting protons across the cell membrane and uncoupling the transmembrane pH gradient from energy-requiring processes but is significantly less potent as a growth inhibitor (Freese, 1978; Kabara, 1978; McLaughlin & Dilger, 1980). It has been shown that growth inhibition in the presence of saturated fatty acids increases with decreasing pH of the medium and is reversible (Freese, 1978). When the bacterial cells are resuspended in a fresh medium, growth does resume. Irreversible disruption of the cell membrane occurs only at a much higher concentration than that required for reversible growth inhibition and takes place more readily with longer chain fatty acids (Freese, 1978). Therefore, the addition of low concentrations of octanoate to a suspension of *S. aureus* is an effective way of altering and studying the effects of intracellular pH without killing the cells.

During the course of the NMR study, several observations led us to conclude that paramagnetic ions are accumulated by the *S. aureus* cells during growth. This was reflected in variations of the line widths and chemical shifts of the intracellular orthophosphate and lactate resonances during anaerobiosis. The magnitudes of these changes were found to be dependent upon the state of oxygenation of the cells. It has been proposed that manganese, in association with superoxide dismutase or with low-molecular-weight negatively charged ligands, may be involved as a defense against oxygen toxicity in a variety of microorganisms (Archibald & Fridovich, 1981a,b). Our objective was to determine whether the presence of manganese in *S. aureus* could account for the NMR results. Accordingly, we utilized ESR in conjunction with NMR to establish the identity and concentration of the paramagnetic ions and to assess the role of these ions.

Materials and Methods

Ninety-percent-enriched [1-^{13}C]glucose and [6-^{13}C]glucose were purchased from Stohler Isotope Chemicals and Cambridge Isotope Laboratories, respectively, and used without further purification. The extent of ^{13}C enrichment and purity were checked by ^{1}H and ^{13}C NMR.

Staphylococcus aureus, strain ATCC 25923, was grown aerobically at 37 °C and pH 7.4 in 1-L batches of a brain heart infusion broth (DIFCO). The growth medium contains infusions from calf brains and beef heart, proteose peptone, glucose, sodium chloride, and disodium phosphate. The cells were collected at late log phase by low-speed centrifugation at 4 °C and washed twice in a cold 200 mM phosphate buffer (6:4 Na_2HPO_4–KH_2PO_4) at pH 7.0. The pellets were subsequently washed and suspended in an equal volume of a pH 6.0 buffer (see below). This resulted in a cell density after resuspension of $\sim 10^{11}$ cells/mL as determined by serial dilutions and plate counts. The intracellular volume was determined by using a value of 1.55 μL/mg dry weight of cells (Kashket, 1981) and was estimated to occupy 16–20% of the total volume. For the ^{31}P NMR experiments, the suspension buffer consisted of 160 mM Mes [2-(*N*-morpholino)ethanesulfonate], 80 mM Pipes [piperazine-*N*,*N*′-bis(2-ethanesulfonate)], 1 mM Na_2HPO_4, 1 mM KH_2PO_4, and 85 mM NaCl. The phosphate concentration was increased to 20 mM (1:1 Na_2HPO_4–KH_2PO_4) for the ^{13}C NMR measurements. The pH of each suspension was adjusted to the desired value by the addition of 0.1 N HCl or NaOH. pH measurements were made at ambient temperature with a Corning 130 digital pH meter calibrated against standard buffers.

Cell extracts were prepared by adding 60% cold perchloric acid (6% final concentration) to the cell suspension and mixing for 5 min. The cellular debris was removed by centrifugation and the supernatant neutralized by adding concentrated NaOH. In order to extract the teichoic acid from the cell walls, the pellet was resuspended in a 0.2 N NaOH solution at ambient temperature and stored under nitrogen (Hughes & Tanner, 1968). After 1 h, the suspension was centrifuged again to remove the solid material. The alkaline-soluble fraction was then examined by ^{31}P NMR.

NMR spectra of intact cells were measured at 20 °C under anaerobic conditions. The cell suspensions were incubated in the probe of the NMR spectrometer and in capped sample tubes during the accumulation of spectra. Sample spinning was employed in order to improve resolution. In separate experiments, the suspensions were bubbled vigorously with O_2 for 1–2 min outside the magnet. NMR spectra were obtained with the samples in capped tubes as a function of time after oxygenation, during which the cells became anaerobic. The minimum time elapsed after oxygenation of the cells, and the measurement of a spectrum was 2 min. Therefore, the spectra at the outset were obtained under partially aerobic conditions.

^{31}P NMR spectra were measured at 109.2 and 121.5 MHz on a JEOL FX-270 (10-mm diameter tube) and a Bruker CXP-300 (20-mm diameter tube) operating in a Fourier transform mode. Neither field/frequency lock nor proton decoupling was used. Typically, spectra were accumulated in 3–4 min by using 40° pulses and 0.25-s repetition times. All chemical shifts are expressed relative to external 85% phosphoric acid. A peak appearing at 0.60 ppm and assigned to teichoic acid was used in all cases as an internal chemical shift reference. The intra- and extracellular pHs were determined by using the chemical shifts of the orthophosphate resonances (P_i) and NMR titration curves of P_i measured in the suspending buffer and cell digest. The digest for the pH titration curve was prepared by lysing the cells with lysostaphin obtained from Sigma Chemical Co. Intact cells were suspended in distilled water containing 20 units/mL lysostaphin. The reaction mixture was then incubated at pH 7.0 and 37 °C for 5 h and centrifuged at 130000*g* for 1 h. The pH of the supernatant was adjusted to the desired value by addition of 0.1 N HCl or NaOH.

Broad band proton-decoupled ^{13}C NMR spectra were obtained at 67.8 and 75.5 MHz in 5- and 10-mm sample tubes on the FX-270 and CXP-300 spectrometers, respectively. The spectra were recorded as a function of time after the addition of [1-^{13}C]- or [6-^{13}C]glucose by using 60° pulses, 0.7–1.0-s repetition times, and 200–800 scans. Chemical shifts are given relative to external tetramethylsilane (Me_4Si).

ESR data were recorded at X band (9.5 GHz) on a Varian E-9 spectrometer by using a dual rectangular cavity and an aqueous solution flat cell. Measurements of *g* values and intensities were done with DPPH ($g = 2.0036$) as a standard.

Results

^{31}P NMR Measurements. Figure 1 shows a series of ^{31}P NMR spectra of *S. aureus* cells suspended in a pH 6.0 buffer and in the absence of a carbon source. The spectrum in Figure 1a was obtained within 5 min after the final suspension of the cells. On the basis of their chemical shifts, the peaks at 2.47 and 1.28 ppm are assigned to the intracellular (P_i^{in}) and extracellular (P_i^{ex}) orthophosphate, respectively. The chemical shift difference of the two peaks is primarily due to an arti-

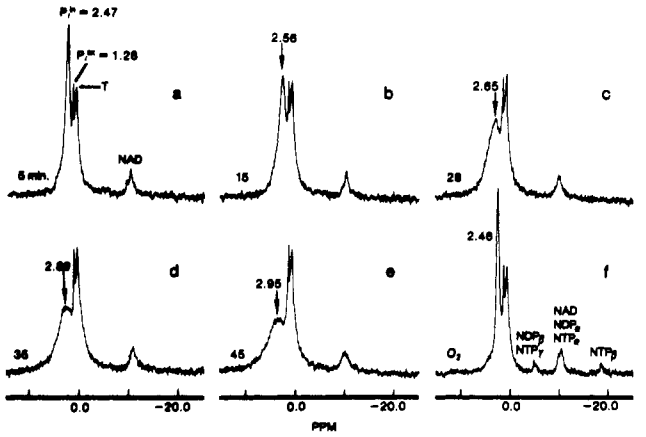

FIGURE 1: 121.5-MHz ^{31}P NMR spectra of *S. aureus* cells grown in brain heart infusion (BHI) broth and suspended in a pH 6.0 buffer. The cell density used in the NMR experiments is $\sim 10^{11}$ cells/mL. Each spectrum consists of 800 scans measured in approximately 3 min and at 20 °C: (a–e) Spectra obtained under anaerobic conditions as a function of time after suspension of the cells in the buffer; (f) cells shown in (e) were vigorously oxygenated for 1–2 min, and the spectrum was recorded within 5 min after placing the sample tube in the magnet. In (a), T = teichoic acid.

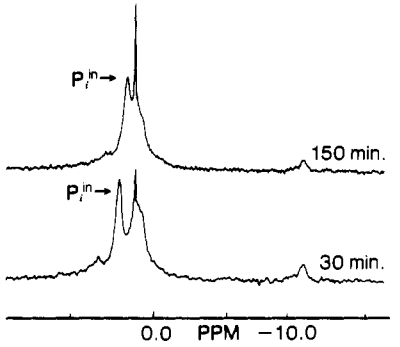

FIGURE 2: 109.2-MHz ^{31}P NMR spectra of anaerobic *S. aureus* cells at 20 °C as a function of time after suspension in a pH 6.0 buffer. The cells were grown in BHI containing 0.4 mM EDTA.

ficially imposed transmembrane pH gradient (Δ pH $\sim$1.0), since the cells were grown aerobically at pH 7.4 and suspended in the pH 6.0 buffer.

The resonance at 0.60 ppm, with a 70-Hz line width at half-height, is characteristic of a phosphodiester (Gadian et al., 1979). Its chemical shift in isolated cell walls (see below) remains constant between pH 3 and pH 8. We have also observed this resonance in the ^{31}P NMR spectrum of Gram-positive *Bacillus subtilus* but not in those of Gram-negative *Escherichia coli* or *Pseudomonas aeruginosa*. In order that we could establish the origin of the peak, *S. aureus* cells were lysed with perchloric acid and centrifuged. The ^{31}P NMR spectrum of the supernatant consisted of a single resonance due to the orthophosphate; however, the spectra of the pellet suspended in fresh buffer and the alkaline-soluble fraction of this suspension contained, in addition, the resonance at 0.60 ppm. The above results indicate that this signal arises from teichoic acid, a polymer of ribitol or glycerol residues linked through phosphodiester bridges and derived from the cell walls or membranes of Gram-positive bacteria (Sanderson et al., 1962; De Boer et al., 1976; Tarelli & Coley, 1979). The complex of teichoic acid with peptidoglycan can contribute as much as 60% of the cell dry weight.

^{13}C NMR has been previously utilized to elucidate the structures of *S. aureus* cell wall polymers (Tarelli & Coley, 1979). Observation of the alkaline-soluble teichoic acid by ^{31}P NMR, in the present study, indicates a high degree of mobility in the backbone of this polymer. This is consistent with the ^{15}N NMR spectra of labeled Gram-positive bacteria, in which the resonances due to the teichoic D-alanine, teichuronic acetamido and peptidoglycan acetamido, amide, peptide, and free amino residues were identified and used to probe the dynamic properties of cell walls (Lapidot & Irving, 1979a). Of course, the advantage of utilizing ^{31}P NMR is that the metabolic state of the intact cells can be monitored simultaneously.

As shown in Figure 1a–e, the intracellular orthophosphate peak (P_i^{in}) becomes progressively broader when the suspension of *S. aureus* is maintained in an anaerobic environment. Within 1 h, the line width increases severalfold from $\sim$65 to 400 Hz. In addition, the P_i^{in} shifts downfield from 2.47 to 2.95 ppm. Oxygenation of the starved cells results in a significant narrowing and an upfield shift of P_i^{in} to 2.46 ppm (Figure 1f). Additional peaks due to nucleoside di- and triphosphate appear in the spectrum of the oxygenated cells as a result of endogenous metabolism (Ugurbil et al., 1978a). These resonances, identified in Figure 1f, ultimately disappear as long as no carbon source or additional oxygen is introduced. Similar results were obtained when the cells were suspended in pH 7.0 and pH 8.0 buffers, with P_i^{in} appearing at 2.75 and 2.86 ppm, respectively, before the onset of broadening. P_i^{in} shifts downfield from 2.47 to 2.86 ppm, and the cytoplasmic compartment becomes more alkaline as the pH of the external medium increases from 6.0 to 8.0. The intracellular pH is undoubtedly influenced by the pH of the surrounding medium.

The sequence of increasing P_i^{in} line width and chemical shift in the anaerobic suspension of cells followed by a narrowing and upfield shift upon oxygenation can be repeated several times. Throughout this time period, the line width and chemical shift of the extracellular orthophosphate resonance (P_i^{ex}) are virtually unchanged. This is in contrast to the ^{31}P NMR spectra of *E. coli* (Ugurbil et al., 1978a, 1982) in which the line width of P_i^{in} as well as the line width and chemical shift of P_i^{ex} remain constant even when the cells are grown in the brain heart infusion broth (F. S. Ezra et al., unpublished results).

The question of line broadening and downfield shift of P_i^{in} in *S. aureus* was further pursued by growing cells in a brain heart infusion broth containing 0.4 mM EDTA. Even though this concentration of EDTA in the medium was inhibitory, a sufficient cell density was achieved during growth for the NMR experiments. The ^{31}P NMR spectra of the 0.4 mM EDTA grown cells are shown in Figure 2 as a function of time after suspension in the pH 6.0 buffer and storage in a capped NMR tube. Clearly, the P_i^{in} resonance remains narrow, suggesting that the broadening and chemical shift variations observed in Figure 1 are due to a binding of the orthophosphate to paramagnetic metal ions which are accumulated in the cytoplasm during growth (Silver, 1978). The binding must be perturbed each time the cells are bubbled with oxygen in order to account for the P_i^{in} line narrowing and upfield shift (Archibald & Fridovich, 1981a,b). Moreover, the metal ions must remain inaccessible to the surrounding medium. Otherwise, the P_i^{ex} resonance also would be broadened in their presence.

The gradual upfield shift of P_i^{in} from 2.3 to 1.8 ppm and diminution of the pH gradient in Figure 2 indicate an increasingly acidic intracellular environment. A similar collapse of the pH gradient and lack of pH homeostasis in the absence of a fermentable carbon source have been observed by ^{31}P NMR in anaerobic suspensions of *E. coli* (Ugurbil et al., 1978a, 1982). Chelation of the paramagnetic ion species with

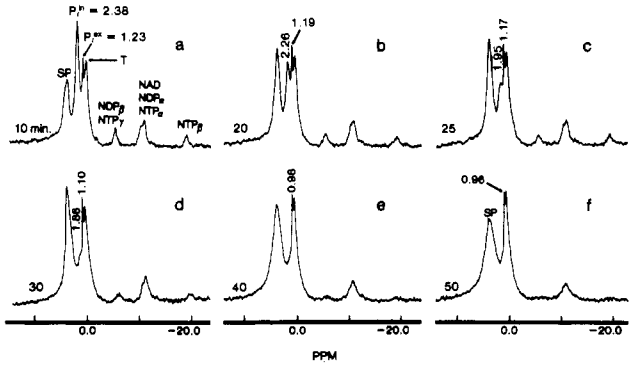

FIGURE 3: 121.5-MHz ^{31}P NMR spectra of glycolyzing *S. aureus* cells. At time zero, the cells were oxygenated, and glucose was added to the suspension to a 50 mM final concentration. Spectra were recorded at 20 °C with the sample in a capped NMR tube. Other experimental conditions are identical with those in Figure 1. In (a), T = teichoic acid, and SP = sugar phosphate.

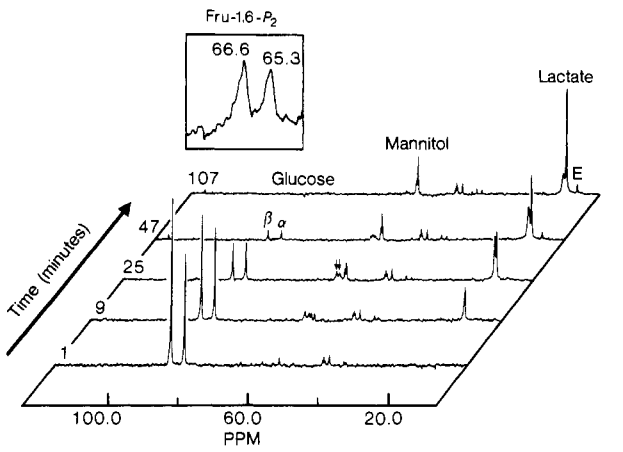

FIGURE 4: 75.5-MHz proton-decoupled ^{13}C NMR spectra of anaerobic *S. aureus* cells at 20 °C as a function of time after the addition of [1-^{13}C]glucose. Cells were suspended in a pH 6.0 buffer. The final concentration of glucose was 50 mM. The arrows in the spectrum obtained at 25 min point to the C-1 (66.6 ppm) and C-6 (65.3 ppm) of β-fructose 1,6-bisphosphate. The insert shows these two resonances on an expanded scale. Fru-1,6-P_2, fructose 1,6-bisphosphate; E, ethanol. The remaining unassigned peaks are due to the buffer.

EDTA, in the present case, may render the cells more permeable to protons and promote rapid acidification of the cytoplasm. In the remaining experiments, therefore, EDTA was not introduced into the growth medium.

When glucose was added to the suspension of cells after the P_i^{in} resonance had become broad, the resonances arising from sugar phosphates, nucleoside di- and triphosphate could not be readily detected due to broadening by the paramagnetic ions. Glycolysis had to be occurring, since the intensity of P_i^{in} did decrease and P_i^{ex} shifted slightly upfield, presumably as a result of the accumulation of organic acids (Ugurbil et al., 1978a). For this reason, glucose was added immediately after suspension of the cells in the buffer. The results are shown in Figure 3. The rapid reduction of the P_i^{in} intensity in Figure 3a, 10 min after the addition of glucose, is accompanied by the appearance of sugar phosphate as well as nucleoside di- and triphosphate. The line widths of these resonances gradually increase with time (Figure 3a–f). Unlike the ^{31}P NMR spectra of *E. coli* which initially exhibit a downfield shift of P_i^{in} during anaerobic glycolysis as a result of ATP hydrolysis (Ugurbil et al., 1978a, 1982), no such shift can be detected in *S. aureus*. Rather, the chemical shift of P_i^{in} decreases monotonically from 2.38 to 1.86 ppm and that of P_i^{ex} decreases from 1.23 to 0.96 ppm. Both compartments become increasingly acidic. The pH of the extracellular space before and after glycolysis is determined from the chemical shifts of P_i^{ex} to be 6.0 and 5.3, respectively. These values are consistent with the readings obtained on a pH meter. The internal pH is more difficult to determine accurately due to the presence of paramagnetic ions in the cytoplasm; however, it should be noted that the chemical shift inequivalence ($\Delta\delta$) between P_i^{in} and P_i^{ex} decreases from 1.15 in Figure 3a to 0.76 ppm in Figure 3d. This is due to a depletion of the transmembrane pH gradient that occurs during glycolysis.

ESR Measurements. ESR spectra of intact *S. aureus* cells were measured, but we were unable to detect the presence of paramagnetic ions, probably due to binding of the ions to negatively charged ligands (Imedidze et al., 1978). An examination of a cell extract in 6% perchloric acid did reveal a sextet pattern characteristic of free Mn(II) hexaquo ions with $g = 2.0090$ and a peak to peak distance of 95 G. When the pH of the extract solution was raised with concentrated NaOH, the ESR signal was markedly reduced and barely detectable above pH 6.0.

The concentration of Mn(II) in the extract was estimated from the ESR spectrum to be $\sim 1 \times 10^{-5}$ M. Since the cytoplasmic volume in the intact cellular suspension occupies approximately 20% of the total volume and further dilution occurs during perchloric acid extraction, the total concentration of the manganese ions inside the cells is at least 5-fold higher.[2] A fresh solution of the growth medium in 6% perchloric acid and at 10× the normal concentration was also examined by ESR. It was found to contain only trace amounts ($\sim 1 \times 10^{-6}$ M) of Mn(II) ions, significantly less than that detected in the extract. Therefore, it is apparent that manganese is actively accumulated by the cells during growth.

^{13}C NMR Measurements. Figure 4 shows a sequence of ^{13}C NMR spectra of an anaerobic suspension of *S. aureus* cells measured as a function of time after the addition of 1-^{13}C-enriched glucose. The resonances have been assigned on the basis of chemical shift information, known metabolic pathways, and a comparison with previous NMR studies on *Saccharomyces cerevisiae* and *E. coli* (den Hollander et al., 1979; Ugurbil et al., 1978b). As can be seen, the β-anomer of [1-^{13}C]glucose is consumed more rapidly than the α-anomer. The consumption of glucose is accompanied by the appearance of three end products with resonances at 17.6, 20.5 (two peaks), and 63.9 ppm and a transient intermediate at 65.3 and 66.6 ppm. Identical results were obtained when [6-^{13}C]glucose was used as the carbon source. The resonance at 17.6 ppm is due to the C-2 of ethanol whereas the two peaks in the 20.5 ppm region are assigned to the C-3 of intra- and extracellular lactate. The assignments of the two lactate peaks are discussed in greater detail below.

The resonance at 63.9 ppm, characteristic of a hydroxymethyl carbon, could not be assigned to any products of the Embden–Meyerhof pathway. Its chemical shift was unchanged irrespective of whether [1-^{13}C]- or [6-^{13}C]glucose was used. The chemical shift of the protons directly linked to this carbon was determined from a selectively proton-decoupled ^{13}C NMR spectrum to be 3.85 ppm downfield from (trimethylsilyl)propionate (TSP). When a suspension of whole

[2] In vivo, manganese exists in several valence states (Archibald & Fridovich, 1981a,b). The P_i^{in} line broadening is attributed mainly to manganous ions. Mn(III) does not give rise to an observable ESR signal due to its short electron relaxation time and is not expected to induce significant broadening of the orthophosphate resonance (Eaton, 1965); however, it is reduced to Mn(II) during perchloric acid extraction. This suggests that the relative concentration of the two species, in vivo, is dependent upon the state of oxygenation of the cells.

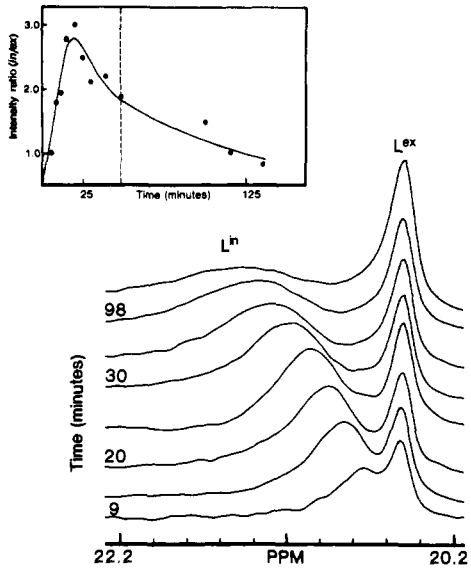

FIGURE 5: Lactate region (20.2–22.2 ppm) of the proton-decoupled ^{13}C NMR spectra of glycolyzing *S. aureus* cells as a function of time. The spectra were obtained from the same experiment as in Figure 4. The insert shows the time course of the intracellular/extracellular lactate integrated intensity ratio. Glucose consumption is completed at ~50 min (vertical dashed line). L^{in}, intracellular lactate; L^{ex}, extracellular lactate.

cells was centrifuged, the peak appeared in the spectrum of the pellet resuspended in fresh buffer but not in that of the supernatant solution. This observation suggested an intracellular metabolite as the origin of the peak. Besides resonances from lactate and ethanol, the ^{13}C NMR spectrum of a perchloric acid extract (not shown) exhibited an intense peak at 63.9 ppm and two considerably weaker signals due to unenriched oxygen-linked methine carbons at 70.2 and 71.5 ppm. By comparison with the spectra of polyols, these peaks were assigned to ^{13}C-1/C-6 (63.9 ppm), C-3/C-4 (70.2 ppm), and C-2/C-5 (71.5 ppm) of mannitol. The identity of the metabolite was subsequently confirmed by adding a sample of mannitol to the extract.

In addition to the end products, two peaks of equal intensities are observed in Figure 4 at 66.6 and 65.3 ppm, slightly downfield of the mannitol peak at 63.9 ppm. This region of the spectrum obtained at 25 min after the addition of glucose is shown on an expanded scale in the insert. The two resonances assigned to C-1 and C-6 of β-fructose 1,6-bisphosphate (den Hollander et al., 1979) increase to a maximum intensity between 9 and 25 min and eventually disappear from the spectra. Identical results were obtained with [6-^{13}C]glucose. Evidently, a ^{13}C label introduced at C-1 or C-6 is distributed equally between the two sites. As described by Shulman and co-workers (Ugurbil et al., 1978b; den Hollander et al., 1979), this is due to scrambling of the label at the triosephosphate isomerase level and a back-synthesis of fructose 1,6-bisphosphate (Fru-1,6-P_2) from dihydroxyacetone phosphate and glyceraldehyde 3-phosphate through aldolase. Under our experimental conditions, these reactions are fast compared to the rate of glycolysis, allowing complete scrambling to take place.

Closer examination of the ^{13}C NMR spectra in Figure 4 reveals the presence of two distinct peaks in the lactate region. These two peaks are plotted on an expanded scale in Figure 5. The high-field resonance at 20.5 ppm remains constant whereas the low-field resonance shifts downfield from 20.7 to 21.4 ppm during glycolysis. Concurrently, the line width increases severalfold from 22 to 68 Hz. The following experimental results were used in assigning the low-field resonance to intracellular lactate (L^{in}) and the high field to extracellular lactate (L^{ex}). First, the ^{13}C NMR spectrum of the cell extract showed only one resonance at 20.5 ppm in this chemical shift region. A spectrum of the supernatant obtained by centrifuging the cells after the completion of glycolysis also exhibited one peak at 20.5 ppm; however, when the pellet was resuspended in fresh buffer, two peaks were once more detected. When the pH of the medium was abruptly decreased from 6.0 to 3.5 by adding 1.0 N HCl to the cell suspension, the low-field resonance remained constant whereas the high-field resonance shifted upfield from 20.5 to 20.1 ppm. The C-3 lactate peak is expected to shift upfield with increasing acidity in the region of the p*K*. Finally, the addition of $MnSO_4$ caused the disappearance of the peak at 20.5 ppm, but the signal was restored when EDTA was subsequently added to the suspension. The low-field peak, in contrast, was unaffected by the $MnSO_4$ or EDTA.

A plot of the L^{in}/L^{ex} integrated intensity ratio as a function of time is shown in Figure 5 (insert). During the first 20 min, the integrated intensity of L^{in} rapidly becomes greater than that of L^{ex}, and the ratio approaches a maximum value of 3. Thereafter, net efflux of lactate occurs until an L^{in}/L^{ex} intensity ratio of 0.8 is attained at 135 min. This final intensity ratio has values ranging from 0.5 to 1.0 in different suspensions of *S. aureus* which we have examined. It represents the total amount of lactate in each of the two compartments. Since the cytoplasmic compartment in these samples constitutes only ~20% of the total volume, the final concentration of lactate inside the cells is calculated to be from 2 to 5 times the concentration found in the surrounding medium. That is, a lactate concentration gradient favoring the cytoplasmic compartment exists under our experimental conditions. The gradient was found to persist in suspensions that were monitored for as long as 5 h after the addition of glucose. To check for differences in the longitudinal relaxation times (T_1) and the nuclear Overhauser effect (NOE), we measured several ^{13}C NMR spectra at the end of the anaerobic cycle using 30° pulses, 3–6-s pulse repetition times, and gated decoupling. The relative intensities of the lactate resonances in these spectra were comparable (±10%) to those obtained under the more rapid pulsing and continuous broad band decoupling conditions.

When the cells were momentarily bubbled with oxygen, pronounced changes occurred in the two lactate peaks whereas the mannitol and ethanol peaks were unaltered. Parts a and b of Figure 6 show the distribution of lactate following anaerobic glycolysis and within minutes after oxygenation. The L^{in}/L^{ex} integrated intensity ratio increases from 0.8 in Figure 6a to 1.6 in Figure 6b. This provides a direct observation of the uptake of lactate against the concentration gradient established under anaerobic conditions. Oxygenation also causes the line width of L^{in} to decrease to its original value of ~25 Hz and the resonance to shift upfield to 20.9 ppm. L^{in} approaches the chemical shift of L^{ex}, but the two resonances do not completely merge. If the sample is then allowed to revert to an anaerobic state, the intensity of L^{in} decreases and that of L^{ex} simultaneously increases. An L^{in}/L^{ex} intensity ratio of 1.4 is observed in Figure 6c, 15 min after oxygenation of the cells. Concurrently, the L^{in} resonance shifts downfield to 21.0 ppm and tends to broaden, but L^{ex} remains constant at 20.5 ppm.

The effects of two additional oxygenation cycles followed by anaerobic incubation are shown in Figure 6d–i. As is illustrated in Figure 6d,g, 4–7 min after the cells are bubbled with oxygen, the lactate is predominantly concentrated inside

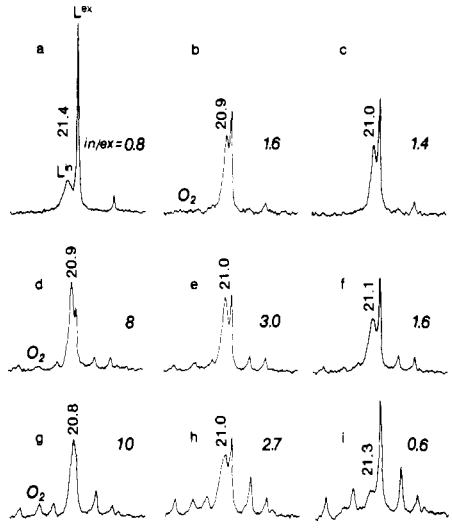

FIGURE 6: Effect of oxygenation on the intra- and extracellular lactate resonances of *S. aureus* cells. Proton-decoupled ^{13}C NMR spectra were recorded at 20 °C: (a) Lactate region of the spectrum of anaerobic cells measured at 135 min after the addition of glucose. This spectrum was obtained from the same experiment as in Figure 4. (b–i) Three cycles of oxygenation followed by anaerobic incubation. Incubation times after oxygenation during each cycle are as follows: cycle 1, (b) 3 and (c) 11 min; cycle 2, (d) 4, (e) 20, and (f) 36 min; cycle 3, (g) 7 and (h) 27 min and (i) ~14 h (stored at 0 °C). in/ex, internal/external lactate resonance integrated intensities. The unidentified resonances in (g–i) are due to products of respiration. Their assignments are not discussed in this paper.

the cells. The L^{in}/L^{ex} intensity ratio approaches an average value of 9 (±3). During anaerobic incubation, lactate continues to flow into the surrounding medium until an L^{in}/L^{ex} intensity ratio of 0.6 is achieved. Even after 14 h of storage of the cells at 0 °C (Figure 6i), this ratio is sustained. It can also be seen that with each oxygenation cycle L^{in} shifts upfield to 20.8–20.9 ppm and decreases in line width. The situation is reversed in the absence of oxygen. These effects are accompanied by a decrease in the total amount of lactate as a consequence of the cells respiring. Eventually, other resonances due to products of respiration, including amino acids, appear in the ^{13}C NMR spectra (Ugurbil et al., 1978b). The assignments of these resonances are outside the scope of this paper and will not be discussed.

The broadening and chemical shift of the internal lactate resonance in the ^{13}C NMR spectra parallel the trends observed by ^{31}P NMR and once more suggest the presence of paramagnetic ions. Indeed, when [1-^{13}C]glucose was added to a suspension of 0.4 mM EDTA grown *S. aureus*, L^{in} appeared 0.3 ppm downfield of L^{ex}. No further downfield shift or broadening of the internal lactate peak occurred, even up to 3 h after the glucose had been exhausted. It is likely that the difference in the pH of the internal and external compartments contributes to the residual 0.3 ppm chemical shift inequivalence of the two lactate peaks. In a separate experiment, ^{13}C NMR spectra of the control cells (in the absence of EDTA) were also measured at 20 MHz on a CFT-20 spectrometer. No evidence was found for a line width or chemical shift dependence of the lactate resonance on the magnetic field strength that would indicate chemical exchange processes (Martin et al., 1980).

Effects of Octanoate. Prior to studying the effects of octanoate on glucose metabolism and lactate transport, a series of ^{31}P NMR spectra of *S. aureus* were recorded in the presence of varying concentrations of the fatty acid at pH 6.0. This was necessary in order to establish the concentration of acid required for the ^{13}C NMR experiments. The cells were washed and suspended in octanoate-containing buffers. ^{31}P NMR

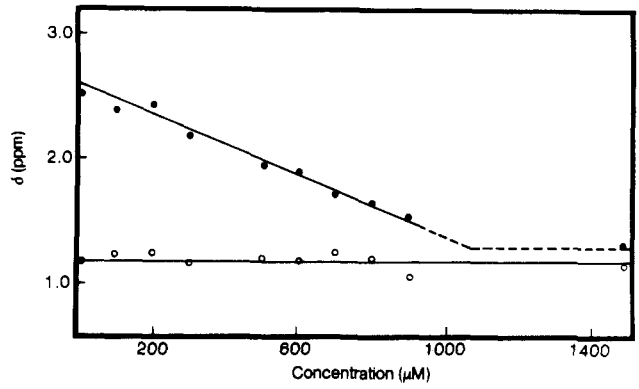

FIGURE 7: Effect of increasing concentrations of octanoic acid (undissociated species) on the chemical shifts of intracellular (●) and extracellular (○) orthophosphate resonances of anaerobic *S. aureus* cells at 20 °C.

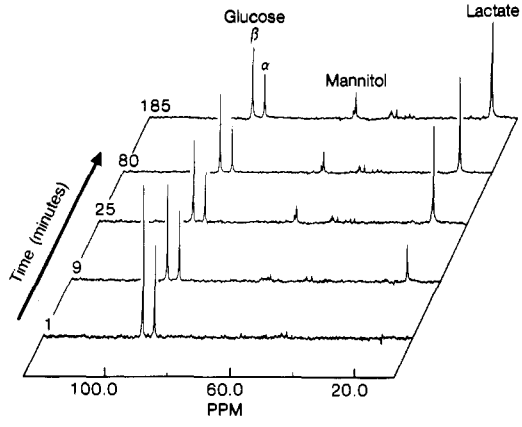

FIGURE 8: 75.5-MHz proton-decoupled ^{13}C NMR spectra of glycolyzing anaerobic *S. aureus* cells as a function of time after addition of [1-^{13}C]glucose (50 mM). The cells were washed and suspended in a pH 6.0 buffer containing 400 μM octanoic acid (5.9 mM octanoate concentration). Other conditions are identical with those in Figure 4.

measurements were made immediately after the final suspension.

Figure 7 is a plot of P_i^{in} and P_i^{ex} chemical shifts as a function of octanoic acid concentration. P_i^{ex} remains constant whereas P_i^{in} shifts upfield toward P_i^{ex} as a consequence of a drop in intracellular pH. At pH 6.0, octanoate exists as a mixture of the neutral carboxylic acid and its anionic counterpart (A^-/HA = 13.8), but it is the acid in its more lipid-soluble neutral form that acts as the protonophore (Freese, 1978; McLaughlin & Dilger, 1980). The neutral species penetrates the cell membrane more readily and is primarily responsible for the growth inhibitory activity (Kabara, 1978). Therefore, the abscissa in Figure 10 refers to the concentration of the undissociated species only. At 1 mM concentration, the chemical shift inequivalence between P_i^{in} and P_i^{ex} (and therefore Δ pH) almost disappears; however, the two P_i resonances do not coalesce even at 1.5 mM octanoic acid. The residual 0.15 ppm chemical shift separation is either due to a difference in the ionic strength of the cytoplasmic and extracellular compartments or is caused by binding of paramagnetic metal ions to the intracellular orthophosphate (Roberts et al., 1981).

Figure 8 shows a series of ^{13}C NMR spectra of *S. aureus* suspended in a buffer containing 400 μM octanoic acid. The spectra were otherwise obtained under conditions identical with those in Figure 4. The concentration of octanoic acid was chosen to be approximately 40% of that required to cause a complete collapse of the pH gradient. The main features of

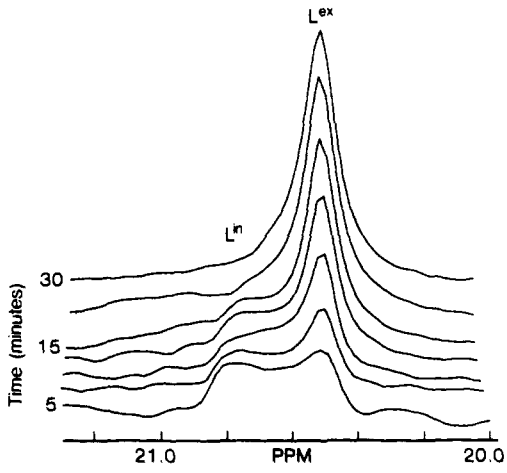

FIGURE 9: Lactate region of the proton-decoupled ^{13}C NMR spectra of anaerobic *S. aureus* cells during glycolysis in the presence of 400 μM octanoic acid. The spectra were obtained from the same experiment as in Figure 8.

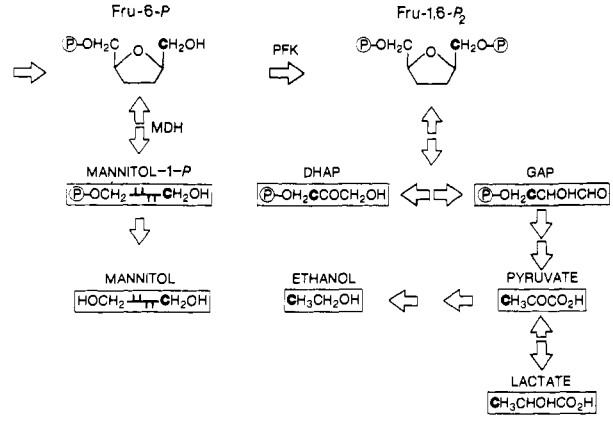

FIGURE 10: Partial scheme for pathways involved in anaerobic metabolism of glucose by *S. aureus* cells. The pathway for synthesis of mannitol has been previously proposed by Edwards et al. (1981). Fru-6-P_2, fructose 1,6-bisphosphate; GAP, glyceraldehyde 3-phosphate; DHAP, dihydroxyacetone phosphate; PFK, phosphofructokinase; MDH, mannitol-1-phosphate dehydrogenase.

the spectra are the resonances due to fructose 1,6-bisphosphate, mannitol, and lactate. No difference in the rate of utilization of the α- and β-glucose is observed. During the first 20 min, the rate of glucose consumption is only slightly retarded in the presence of octanoic acid relative to that of the control cells shown in Figure 4. Thereafter, no glucose is consumed even up to 185 min after its addition to the suspension of cells.

Figure 9 shows the lactate region of the ^{13}C NMR spectra on an expanded scale. The intra- and extracellular peaks can be clearly resolved due to a 0.3 ppm chemical shift separation. Although the intensities are equal in the first 5 min after the onset of glycolysis, most of the lactate rapidly leaks out of the cells. By 15 min, the intensity ratio of the internal to external lactate is 0.2, approximating the ratio of the cytoplasmic to external volume. The internal lactate resonance is not observable after 20 min, even though no measurable broadening of this peak occurs. Instead, L^{in} shifts upfield and eventually merges with L^{ex}. When the cells are oxygenated (data not shown), neither uptake nor consumption of lactate is detected.

Discussion

Distribution of End Products and Rate of Glycolysis. The series of reactions involved in the anaerobic metabolism of glucose and relevant to the present discussion is shown in Figure 10. The appearance of lactate in Figure 4 as the major end product is consistent with previous studies (Blumenthal, 1972). On the other hand, the accumulation of mannitol as an intracellular product of glucose metabolism has only recently been reported in a study utilizing gas–liquid chromatography and mass spectrometry (Edwards et al., 1981). It has been suggested that mannitol acts either as an electron sink, a storage carbohydrate, a source of NADPH, or an osmoregulator, the latter accounting for the high salt tolerance of *S. aureus*. The most likely pathway proposed for its formation involves the conversion of fructose 6-phosphate (Fru-6-P) to mannitol 1-phosphate (Mno-1-P). The Mno-1-P is subsequently dephosphorylated through a phosphatase or a phosphotransferase enzyme system to mannitol. As illustrated in Figure 10, Fru-6-P appears as the common intermediate for the two competing metabolic pathways leading to the formation of Fru-1,6-P_2 and Mno-1-P. Therefore, any parameter that can preferentially influence the activity of one or more of the enzymes involved in these pathways can alter the final distribution of mannitol and lactate. The pH of the medium does in fact have a profound effect on the amount of mannitol that is produced by the cells. We will return to a discussion of this point shortly.

It is important to note that in the present study, the rate of glucose utilization is considerably lower than that reported for *E. coli* (Ugurbil et al., 1978b). Yet, it is sufficiently rapid to reveal the preferential consumption of the β-anomer. Complete equilibration of the ^{13}C label between the C-1 and C-6 positions of fructose 1,6-bisphosphate also is evident in *S. aureus* whereas a minimal amount of scrambling was observed with *E. coli*. These results are not unexpected, since the *E. coli* were suspended in a pH 7.4 alkaline medium compared to the pH 6.0 buffer used in this work. In addition to altering the distribution of end products, there is growing evidence that the pH of the incubating medium influences the intracellular pH which in turn can control the rate of glycolysis in bacterial cells (Ogino et al., 1980; Padan et al., 1981; Foyer et al., 1982). Specifically, it has been proposed that low intracellular pH leads to a reduced glycolytic activity (Roos & Boron, 1981). Shulman and co-workers calculated the pH profile of glycolysis in *E. coli* from ^{31}P NMR spectra and pointed out its similarity to the pH–rate profile of phosphofructokinase (PFK), implying that the control of glycolysis by pH may be due to the regulation of PFK activity (Ugurbil et al., 1978a). On the contrary, glucose uptake rates in *S. cerevisiae* yeast cells were found not to differ significantly between pH 5.5 and pH 7.0 (den Hollander et al., 1979), a result that is consistent with the fact that the yeast cells are capable of growing over a wider range of pH values than the bacterial cells.

To ascertain the role of pH in *S. aureus*, intact cells were suspended separately in pH 6.0 and pH 7.5 buffers and examined by ^{13}C NMR after the addition of glucose. From the ^{31}P NMR spectra of the starved cells, the initial intracellular pH values in these two suspensions are estimated to be 6.8 and 7.2, respectively. The results of the ^{13}C NMR experiments at 15 °C are shown in Figure 11. The rate of glycolysis is undoubtedly greater at the higher pH. In addition, the difference in the rates at which the α- and β-anomers are metabolized becomes greatly magnified in the more alkaline medium, with the β-glucose being consumed much more rapidly. The insert in Figure 11 shows the ^{13}C NMR spectra of the intact cells suspended in the pH 6.0 and pH 7.5 buffers after the completion of glycolysis. The ratio of mannitol to lactate produced decreases by 6-fold with increasing pH. In other words, the lower pH favors the formation of mannitol.

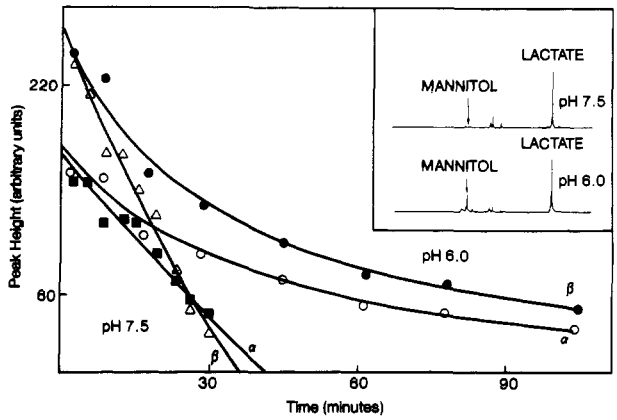

FIGURE 11: Time course of the α- and β-glucose consumption by *S. aureus* cells suspended in pH 6.0 and pH 7.5 buffers. The pH 6.0 buffer is described under Materials and Methods. The pH 7.5 buffer consisted of 200 mM Pipes, 50 mM Mes, 85 mM NaCl, 10 mM Na_2HPO_4, and 10 mM KH_2PO_4. Spectra were measured at 15 °C. The insert on the upper right-hand corner shows the final spectra obtained from the anaerobic *S. aureus* cells after the completion of glycolysis. The unassigned peaks are due to the buffers.

This could very well be the reason that higher levels of mannitol have been found in anaerobic and semianaerobic *S. aureus* (Edwards et al., 1981). The intracellular pH may be lower under these conditions relative to the aerobically grown cells. A consideration of the pathways shown in Figure 10 suggests that the lower intracellular pH leads to a reduced PFK activity, an increase in the flow of glucose through Mno-1-P dehydrogenase (MDH), and an increase in the final concentration of mannitol.

The conversion of Fru-6-P to Fru-1,6-P_2 (PFK activity) is not necessarily the sole locus along the glycolytic pathway that is influenced by the pH of the medium. The phosphoenolpyruvate:sugar phosphotransferase system (PTS), which catalyzes the transport and phosphorylation of glucose in *S. aureus* by group translocation, may also be sensitive to pH (Reider et al., 1979; Dills et al., 1980; Robillard & Konings, 1981). The initial rate of glycolysis in *S. aureus* in the presence of octanoate is slightly less than that of the control cells; however, metabolic activity ceases midway during glycolysis (see Results). In contrast, the addition of uncouplers to *E. coli* has been found either to stimulate or to have a negligible effect on the uptake of PTS sugars (Reider et al., 1979). The abrupt decrease in the glycolytic rate of octanoate-suspended *S. aureus* is then very likely pH induced. As glycolysis progresses between 0 and 20 min, both intracellular and extracellular compartments become more acidic (Figure 3). This serves to drive the transport of the uncoupler into the cytoplasm (Cramer & Prestegard, 1977). Lowering of the external pH, in effect, increases the concentration of the octanoic acid in its lipid-soluble protonated form. Consequently, the internal pH approaches that of the external medium with increasing octanoic acid (Figure 7), resulting in the inhibition of glycolysis.

We considered the possibility of pH impairing glucose-phosphate isomerase activity. This would result in the accumulation of glucose 6-phosphate (Glc-6-P) as an end product of glycolysis in the presence of octanoate. The C-1 resonance of Glc-6-P cannot be resolved from the C-1 of glucose in the ^{13}C NMR spectra of intact cells. Any buildup of the phosphorylated metabolite therefore would appear as a leveling off in the rate of glucose consumption as shown in Figure 8. To eliminate this possibility, a similar series of spectra were obtained with [6-^{13}C]glucose used as the carbon source. A resonance from the C-6 of Glc-6-P would be expected to appear at 64.3 ppm. In fact, no accumulation of [6-^{13}C]Glc-6-P or other metabolic intermediates could be detected. The implication is that, in addition to altering the PFK activity which is reflected in the level of mannitol produced, the pH controls the rate of PTS-mediated glucose uptake and phosphorylation by the cells.

Lactate Transport. The appearance of two distinct lactate resonances in the ^{13}C NMR spectra of *S. aureus* (Figure 5) allows the determination of the distribution of this metabolite in the cytoplasm and in the external medium. A general NMR method of studying transport in cells using spin-echo techniques has been recently described (Brindle et al., 1979). It relies on a difference in the magnetic susceptibility in order to distinguish molecules inside and outside the cells. In more specific cases, chemical shift differences arising from transmembrane pH gradients were used to study the transport of carboxylic acids into vesicles by ^1H NMR (Cramer & Prestegard, 1977) and to follow the uptake of [2-^{13}C]succinate in *E. coli* by ^{13}C NMR (Ugurbil et al., 1982). Proton correlation and ^{13}C NMR have also been utilized to monitor the accumulation of pyruvate in suspensions of *E. coli* (Ogino et al., 1980) and *Trypanosoma brucei gambiense* (Mackenzie et al., 1982). In the latter two studies, only the NMR signal from the extracellular metabolite was detected. The intracellular resonance was broadened beyond detection and observed only after acid treatment. The manganese-induced chemical shift inequivalence of the two lactate peaks in *S. aureus*, reported in this work, permits the internal and external components to be monitored independently.

In Figure 5 (insert), the integrated intensity of the internal lactate is initially equal to but rapidly becomes greater than that of the external lactate. The rate of production of this metabolite is more rapid than the efflux. The internal/external lactic acid concentration ratio increases from ~5 at 5 min to ~15 at 20 min. These values were calculated by taking into account the 0.2 internal/external volume ratio and assuming that all of the internal component is observable. Rapid efflux occurs between 20 and 135 min, and the concentration ratio decreases from 15 to 4. Clearly, a concentration gradient is maintained during this time period, but the magnitude depends critically on the metabolic state of the cells.

Figure 6 shows the effects of *S. aureus* being subjected to several oxygenation cycles followed by anaerobic incubation and the resulting variations in the distribution of intra- and extracellular lactate. Each time the cells are oxygenated, lactate is transported into the cells. This process requires energy and is presumably driven by the protonmotive force (Matin & Konings, 1973; Kang, 1978). Of course, the final internal/external lactate distribution depends largely on the extent of oxygenation. In Figure 6d,g, the maximum internal/external intensity ratio is measured to be 9 (±3), which is equivalent to a 40–50/1 concentration gradient. The influx is followed by a net efflux of lactate into the external medium as the oxygen is depleted. The concentration gradient ultimately drops to a value of 3, favoring the intracellular compartment.

The observed effects of octanoate provide evidence that the pH also can play a crucial role in the regulation of the transport and distribution of lactate. The collapse of the transmembrane pH gradient in the presence of increasing concentrations of octanoic acid occurs with the cytoplasmic pH approaching that of the surrounding medium (Figure 7). In addition, the accumulation of intracellular lactate is inhibited during anaerobic glycolysis (Figure 9). When the cells are oxygenated, neither uptake nor metabolism of lactate such

as that shown for the control cells in Figure 6 can be detected. In summary, octanoic acid appears to prevent the uptake of the lactate into the cells by promoting the collapse of ΔpH and acidification of the intracellular compartment. Similar effects of the uncoupler 2,4-dinitrophenol on pyruvate transport in *E. coli* have been reported and attributed to a regulation by the pH of the medium (Ogino et al., 1980).

Role of Manganese. The evidence presented in this work points to the fact that *S. aureus* actively accumulates and retains a pool of manganese during growth. The presence of Mn(II) ions is very likely the source of line broadening and shifts observed in the ^{31}P and ^{13}C NMR spectra of energy-depleted and glycolyzing cells. More importantly, the narrowing line width and upfield shift of the intracellular orthophosphate and lactate resonances whenever the cells are oxygenated suggest that manganese may be involved in oxygen metabolism, either directly or indirectly via changes induced in the intracellular pH (Imedidze et al., 1978; Archibald & Fridovich, 1981a,b). Further studies on the effects of manganese in a variety of microorganisms are currently under way in our laboratory.

Registry No. D-Glucose, 50-99-7; lactic acid, 50-21-5; octanoic acid, 124-07-2; orthophosphate, 14265-44-2; teichoic acid, 9041-38-7; Mn, 7439-96-5; ethanol, 64-17-5; D-mannitol, 69-65-8; Fru-1,6-P_2, 488-69-7; O_2, 7782-44-7.

References

Archibald, F. S., & Fridovich, I. (1981a) *J. Bacteriol. 145*, 442–451.

Archibald, F. S., & Fridovich, I. (1981b) *J. Bacteriol. 146*, 928–936.

Blumenthal, H. J. (1972) in *The Staphylococci* (Cohen, J. O., Ed.) pp 111–136, Wiley-Interscience, New York.

Brindle, K. M., Brown, F. F., Campbell, I. D., Grathwohl, C., & Kuchel, P. W. (1979) *Biochem. J. 180*, 37–44.

Cohen, J. O., Ed. (1972) *The Staphylococci*, Wiley-Interscience, New York.

Cramer, J. A., & Prestegard, J. H. (1977) *Biochem. Biophys. Res. Commun. 75*, 295–301.

De Boer, W. R., Kruyssen, F. J., Wouters, J. T. M., & Kruk, C. (1976) *Eur. J. Biochem. 62*, 1–6.

den Hollander, J. A., Brown, T. R., Ugurbil, K., & Shulman, R. G. (1979) *Proc. Natl. Acad. Sci. U.S.A. 76*, 6096–6100.

Deslauriers, R., Ekiel, I., Byrd, R. A., Jarrell, H. C., & Smith, I. C. P. (1982) *Biochim. Biophys. Acta 720*, 329–337.

Dills, S. S., Apperson, A., Schmidt, M. R., & Saier, M. H., Jr. (1980) *Microbiol. Rev. 44*, 385–418.

Eaton, D. R. (1965) *J. Am. Chem. Soc. 87*, 3097–3102.

Edwards, K. G., Blumenthal, H. J., Khan, M., & Slodki, M. E. (1981) *J. Bacteriol. 146*, 1020–1029.

Foyer, C., Walker, D., Spencer, C., & Mann, B. (1982) *Biochem. J. 202*, 429–434.

Freese, E. (1978) in *The Pharmacological Effects of Lipids* (Kabara, J. J., Ed.) pp 123–131, American Oil Chemists' Society, New York.

Gadian D. G., Radda, G. K., Richards, R. E., & Seeley, P. J. (1979) in *Biological Applications of Magnetic Resonance* (Shulman, R. G., Ed.) pp 463–565, Academic Press, New York.

Halpin, R. A., Hegeman, G. D., & Kenyon, G. L. (1981) *Biochemistry 20*, 1525–1533.

Hughes, R. C., & Tanner, P. J. (1968) *Biochem. Biophys. Res. Commun. 33*, 22–28.

Imedidze, E. A., Drobinskaya, I. E., Kerimov, T. M., Ruuge, E. K., & Kozlov, I. A. (1978) *FEBS Lett. 96*, 115–119.

Kabara, J. J. (1978) in *The Pharmacological Effects of Lipids* (Kabara, J. J., Ed.) pp 1–12, American Oil Chemists' Society, New York.

Kallas, T., & Castenholtz, R. W. (1982) *J. Bacteriol. 149*, 237–246.

Kang, S. Y. (1978) *J. Bacteriol. 136*, 867–873.

Kashket, E. (1981) *J. Bacteriol. 146*, 369–376.

Kuchel, P. W. (1981) *CRC Crit. Rev. Anal. Chem. 12*, 155–231.

Lapidot, A., & Irving, C. S. (1979a) *Biochemistry 18*, 704–714.

Lapidot, A., & Irving, C. S. (1979b) *Biochemistry 18*, 1788–1796.

Mackenzie, N. E., Hall, J. E., Seed, J. R., & Scott, A. I. (1982) *Eur. J. Biochem. 121*, 657–661.

Martin, M. L., Delpeuch, J. J., & Martin, G. J. (1980) *Practical NMR Spectroscopy*, Heyden, London.

Matin, A., & Konings, W. N. (1973) *Eur. J. Biochem. 34*, 58–67.

McLaughlin, S. G. A., & Dilger, J. P. (1980) *Physiol. Rev. 60*, 825–863.

Nicolay, K., Hellingwerf, K. J., Gemerden, H. V., Kaptein, R., & Konings, W. N. (1982) *FEBS Lett. 138*, 249–252.

Ogino, T., Arata, Y., & Fujiwara, S. (1980) *Biochemistry 19*, 3684–3691.

Paalme, T., Abira, O., & Vilu, R. (1982) *Biochim. Biophys. Acta 720*, 311–319.

Padan, E., Zilberstein, D., & Schuldiner, S. (1981) *Biochim. Biophys. Acta 650*, 151–166.

Reider, E., Wagner, E. F., & Schweiger, M. (1979) *Proc. Natl. Acad. Sci. U.S.A. 76*, 5529–5533.

Roberts, J. K. M., & Jardetzky, O. (1981) *Biochim. Biophys. Acta 639*, 53–76.

Roberts, J. K. M., Jardetzky, N. W., & Jardetzky, O. (1981) *Biochemistry 20*, 5389–5394.

Robillard, G. T., & Konings, W. N. (1981) *Biochemistry 20*, 5025–5032.

Roos, A., & Boron, W. F. (1981) *Physiol. Rev. 61*, 296–435.

Runquist, E. A., Abbot, E. H., Armold, M. T., & Robbins, J. E. (1981) *Appl. Environ. Microbiol. 42*, 556–559.

Sanderson, A., Strominger, J., & Nathenson, S. (1962) *J. Biol. Chem. 237*, 3603–3613.

Scott, A. I., & Baxter, R. L. (1981) *Annu. Rev. Biophys. Bioeng. 10*, 151–174.

Silver, S. (1978) in *Bacterial Transport* (Rosen, B. P., Ed.) pp 221–324, Marcel Dekker, New York.

Tarelli, E., & Coley, J. (1979) *Carbohydr. Res. 75*, 31–37.

Ugurbil, K., Rottenberg, H., Glynn, P., & Shulman, R. G. (1978a) *Proc. Natl. Acad. Sci. U.S.A. 75*, 2244–2248.

Ugurbil, K., Brown, T. R., den Hollander, J. A., Glynn, P., & Shulman, R. G. (1978b) *Proc. Natl. Acad. Sci. U.S.A. 75*, 3742–3746.

Ugurbil, K., Shulman, R. G., & Brown, T. R. (1979) in *Biological Applications of Magnetic Resonance* (Shulman, R. G., Ed.) pp 537–589, Academic Press, New York.

Ugurbil, K., Rottenberg, H., Glynn, P., & Shulman, R. G. (1982) *Biochemistry 21*, 1068–1073.